IJCRT.ORG ISSN : 2320-2882

INTERNATIONAL JOURNAL OF CREATIVE RESEARCH THOUGHTS (IJCRT)

An International Open Access, Peer-reviewed, Refereed Journal

Numerical Investigation of Three-Dimensional Casson Nanofluid Flow over a Rotating Stretching Surface with Joule Heating and Viscous Dissipation

[1] Somalatha. M.T.,[2] Sumithra. R.,

[3a] Mahesh. S., [3b]Nameethasri. M.A.

[1,2,3] Department of UG, PG Studies and Research in Mathematics,

Nrupathunga University, Bengaluru, Karnataka, India.

Abstract

This work delivers a rigorous numerical exploration of three-dimensional **Casson nanofluid flow** over a rotating bi-directional stretching surface, capturing complex non-Newtonian transport phenomena relevant to modern engineering systems. The mathematical model integrates magnetohydrodynamic effects, Joule heating, viscous dissipation, Brownian motion, and thermophoresis within the Buongiorno nanofluid framework to ensure strong physical realism. Through similarity transformations, the governing conservation equations are reduced and efficiently solved using the robust Keller–Box scheme, providing highly accurate computational insights. Parametric analysis reveals that rotation and magnetic forces markedly reshape velocity fields, while viscous and Ohmic heating intensify thermal transport within the boundary layer. Nanoparticle dynamics governed by Brownian diffusion and thermophoresis significantly enhance heat and mass transfer characteristics. The findings demonstrate improved control of thermal performance in complex fluid systems and highlight the sensitivity of transport processes to key dimensionless parameters. Overall, this study offers a reliable theoretical foundation with direct relevance to advanced technologies such as rotating heat exchangers, polymer processing, electronic cooling, and biomedical thermal management.

Keywords: Casson nanofluid , magnetohydrodynamics, Joule heating, viscous dissipation, Brownian motion, thermophoresis.

1.Introduction

The field of non-Newtonian nanofluids, particularly Casson-type fluids, has garnered significant attention due to their enhanced heat transfer capabilities, which are critical in applications ranging from electronic cooling and nuclear reactor safety to polymer extrusion and biomedical devices. Casson fluids, with their yield-stress characteristics, effectively model complex materials such as blood, chocolate, and honey, especially when enriched with nanoparticles for superior thermal management. While two-dimensional analyses are widely available, the complexity of real-world systems such as rotating machinery and magneto controlled surfaces demands studies that incorporate three-dimensional effects, rotation, stretching, magnetic fields, and thermal irreversibilities within a unified framework. Rotational motion introduces Coriolis forces, bi-directional stretching influences boundary-layer thickness, and an applied transverse magnetic field (MHD) generates Lorentz forces that significantly modify the flow structure. Additionally, Joule heating and viscous dissipation are known to produce non-negligible internal energy generation in high-speed or high-field environments, such as electronic cooling, polymer processing, or power generation systems. The Buongiorno model further extends this complexity by accounting for Brownian diffusion and thermophoresis, crucial mechanisms that affect nanoparticle distribution and thus overall thermal efficiency.

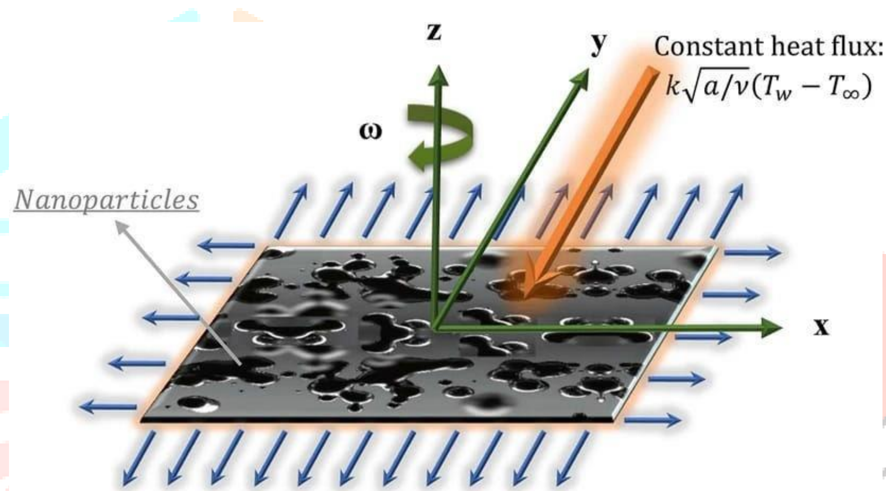

Figure 1:Schematic diagram of the problem under consideration

Figure 1 illustrates the physical configuration of the present problem. The stretching sheet rotates with angular velocity ω along the z-axis, while the x and y axes denote the stretching plane. A constant heat flux is imposed on the surface, represented by $k\sqrt{a/v}(T_w - T_\infty)$. The suspension of nanoparticles within the Casson fluid enhances thermal conductivity, thereby improving heat transfer rates. The outward arrows indicate the fluid motion away from the surface, while the coordinate system highlights the three-dimensional nature of the flow. The inclusion of nanoparticles, Joule heating, and viscous dissipation together provides a realistic framework for simulating thermal fluid processes in rotating machinery, aerospace systems, and modern cooling technologies. Despite extensive research ranging from two-dimensional MHD Casson nanofluid flows on stretching surfaces with radiation and slip conditions to three-dimensional studies involving rotating parallel plates there remains a glaring research gap. Specifically, the interdependence of rotation, bi-directional stretching, MHD, Joule heating, viscous dissipation, and nanoparticle transport in a single three-dimensional Casson nanofluid system has yet to be comprehensively modeled and analyzed. Addressing this gap, our study offers a robust numerical investigation into this coupled system, aiming to deepen physicochemical understanding and support engineering design in advanced thermal systems.

In 1984, Fung explored biodynamic circulatory flow, offering physiological context to non-Newtonian flows. In the year 1991, Andersson and Dandapat laid groundwork for nonNewtonian flow analysis on stretching surfaces. In the year 1994, Gorla and Sidawi contributed free convection models over stretching surfaces. In 1995, Choi and Eastman introduced nanoparticles to enhance thermal conductivity models. In the year 1996, Dash et al. specifically studied Casson flow in porous pipes, and Hassanien analyzed power-law fluid flow over stretching surfaces. In 2004, Sadeghy and Sharifi developed similarity solutions for viscoelastic second-grade fluids over moving plates. In the year 2006, Buongiorno presented a foundational model for convective transport in nanofluids, widely adopted in subsequent research, and Serdar and Dokuz studied three-dimensional stagnation point flows of second-grade fluids. In the year 2007, Sajid et al. developed analytical MHD heat transfer models for third-order fluids, while Aksoy et al. provided boundary-layer equations for modified second-grade fluids. In the year 2008, Shampine and Kierzenka developed a boundary value problem solver relevant to nanofluid simulations. In the year 2009, Sajid et al. worked on unsteady second-grade fluid flow over stretching sheets, and Nield and Kuznetsov examined nanofluid convection in porous media. In the year 2010, Khan and Pop proposed a model for boundary layer nanofluid flow past stretching sheets, while Kuznetsov and Nield incorporated Brownian motion and thermophoresis into nanofluid transport models. In the year 2011, Hayat et al. analyzed unsteady UCM fluid flow with mass transfer effects. In the year 2013, Nadeem et al. examined MHD Casson fluid behavior over porous sheets and also addressed three-dimensional Casson nanofluid boundary-layer flow with convective boundaries. In the year 2014, Pramanik presented Casson flow with thermal radiation over porous exponential stretching surfaces. In the year 2015, Animasaun investigated thermophoresis, variable viscosity, and chemical reactions in MHD dissipative Casson flow. In the year 2016, Shehzad et al. modeled three-dimensional MHD Casson flow in porous media with heat generation, Raju and Sandeep analyzed unsteady Casson-Carreau flow, and Shaw et al. discussed nonlinear convection in Casson fluids over plates with convective boundaries. In the year 2017, Tamoor et al. examined MHD flow of Casson fluid over stretching cylinders, while Gupta and Sharma investigated Casson nanofluid flow with thermal radiation and convective boundary conditions. In the year 2018, Al-Kouz et al. studied heat enhancement in low-pressure nanofluid pipe flows, Zia et al. analyzed three-dimensional Casson flow with cross-diffusion and exponential heat sources, and Bhatti et al. proposed an MHD nanofluid model with gyrotactic microorganisms and chemical reactions. In the year 2019, Prasad et al. explored chemically reactive Casson slip flow over porous sheets, Al-Kouz et al. optimized entropy for nanofluid flow in cavities, and Saeed et al. analyzed thin film Casson nanofluid flow over rotating disks. In the year 2020, Salahuddin et al. studied Casson flow with activation energy, Naga Santoshi et al. investigated Casson-Carreau nanofluid dynamics, Rashidi et al. modeled condensation flow in nanochannels, Mukhtar et al. examined Maxwell nanofluid MHD flow, Yang et al. reviewed nanomaterial-based heating/cooling systems, and Tripathi et al. analyzed Cu-CuO/blood nanofluid flow under magnetic and rotational effects. In the year 2021, Abu-Libdeh et al. studied natural convection of hybrid nanofluids in porous enclosures, Rashidi et al. examined hybrid nanofluid convection in lid-driven cavities, Mahanthesh et al. analyzed dusty nanoliquid flows with quadratic thermal radiation, Alshare et al. studied nanofluid transport in wavy microchannels, and Waqas et al. explored bioconvective nanofluid flow under Darcy-Forchheimer effects. In the year 2022, Zhang et al. used a spectral approach to analyze nonlinear nanofluid flows influenced by Lorentz forces and Arrhenius kinetics, while Wael Al-Kouz and Wahib Owhaib studied radiation effects on rotating Cu-water nanoliquid flow with viscous heating using a modified Buongiorno model, emphasizing entropy generation.

The motivation behind choosing this dissertation arises from the evident research gap in modeling complex, real-world fluid dynamics involving three-dimensional Casson nanofluid flow over a rotating and stretching surface under the simultaneous influence of magnetic fields, Joule heating, viscous dissipation, and nanoparticle transport. While past studies have explored subsets of these phenomena, a unified approach that captures their combined effects is lacking. This dissertation aims to fill that void by developing a robust numerical framework based on the Buongiorno model and Casson fluid theory, facilitating the accurate analysis of coupled momentum, heat, and mass transfer phenomena. The study not only enhances fundamental understanding but also supports the design and optimization of advanced engineering systems such as rotating heat exchangers, electromagnetic cooling devices, polymer extrusion units, biomedical equipment, and aerospace thermal regulators. By conducting a detailed parametric analysis involving key dimensionless numbers like the Casson number (Ca), rotation parameter (Ro), magnetic parameter (M), Brownian motion parameter (Nb), thermophoresis parameter (Nt), and Eckert number (Ec), the dissertation offers valuable insights into thermal and flow behavior optimization. The ultimate objective is to provide a reliable computational model that serves as a benchmark for future research while aiding the development of high-performance, energy-efficient technologies in critical applications where precise control over transport phenomena is essential.

2.Mathematical formulation

This study investigates the laminar, steady-state, three-dimensional flow of an elongated non-Newtonian Casson nanofluid over a rotating surface. The nanofluid surface is subjected to a constant heat flux condition at the boundary. A Cartesian coordinate system is considered, where the flow is aligned along the (x)- and (y)-axes, and the fluid domain occupies the region ($z \geq 0$). The incompressible Casson nanofluid rotates uniformly about the (z)-axis with a constant.

The current problem under investigation governing equations are defined as below

$$\frac{\partial u}{\partial x} + \frac{\partial v}{\partial y} + \frac{\partial w}{\partial z} = 0 \quad (1)$$

$$\rho\left(u\frac{\partial u}{\partial x} + v\frac{\partial v}{\partial y} + w\frac{\partial w}{\partial z} - 2\omega v\right) = \mu\left(1 + \frac{1}{Ca}\right)\frac{\partial^2 u}{\partial z^2} + \sigma {B_0}^2 \quad (2)$$

$$\rho\left(u\frac{\partial u}{\partial x} + v\frac{\partial v}{\partial y} + w\frac{\partial w}{\partial z} + 2\omega u\right) = \mu\left(1 + \frac{1}{Ca}\right)\frac{\partial^2 v}{\partial z^2} + \sigma {B_0}^2 \quad (3)$$

$$\rho Cp\left(u\frac{\partial T}{\partial x} + v\frac{\partial T}{\partial y} + w\frac{\partial T}{\partial z}\right) = k\frac{\partial^2 T}{\partial z^2}\,(\rho Cp)_{np}\left[D_B\left(\frac{\partial T}{\partial z}\frac{\partial C}{\partial z}\right) + \left(\frac{D_B}{T_\infty}\right)\left(\frac{\partial T}{\partial z}\right)^2\right]$$
$$+\mu\left(1 + \frac{1}{Ca}\right)\left[\left(\frac{\partial u}{\partial x}\right)^2 + \left(\frac{\partial v}{\partial y}\right)^2\right] + \sigma {B_0}^2(u^2 + v^2) \quad (4)$$

$$u\frac{\partial C}{\partial x} + v\frac{\partial C}{\partial y} + w\frac{\partial C}{\partial z} = D_B\frac{\partial^2 C}{\partial z^2} + \frac{D_T}{T_\infty}\frac{\partial^2 T}{\partial z^2} \quad (5)$$

where Ca-dimensionless Casson fluid factor, u, v, and w are velocities along x, y and z-directions, $\nu = \frac{\mu}{\rho}$ is the kinematic viscosity, μ is the dynamic viscosity, ρ is the density, T is the temperature, C is the nanoparticle concentration, $\alpha = \frac{k}{\rho Cp}$ is the thermal diffusivity, k is the thermal conductivity, pC_p is the specific heat of the Casson fluid, $(\rho C_p)_{np}$ is the specific heat of the nanoparticles, D_B is the coefficient of Brownian diffusion, D_T is the coefficient of thermo-migration diffusion and T_∞ is the ambient temperature.

The boundary conditions are

$$W = v = 0, u = U_w + ax, -k\left(\frac{\partial T}{\partial z}\right) = q_w, C = C_w \; at \; z = 0$$

$$v = 0, u = 0, T = T_\infty, C = C_w \; as \; z \to \infty \quad (6)$$

where a is stretching rate and $q_w = (T_w - T_\infty)k\sqrt{a/v}$ is constant heat flux. Upon considering

$$u = axf'(\xi), \quad v = axg(\xi), \quad w = -\sqrt{av}f(\xi), \quad \xi = z\sqrt{\frac{u_w}{xv}}$$

$$T = (T_w - T_\infty)\theta(\xi) + T_\infty, C = (C_w - C_\infty)\phi(\xi) + C_\infty \quad (7)$$

Equation (1) is satisfied and the other Eqs. (2)– (6) yield

$$\left(1+\frac{1}{Ca}\right)f''' + ff'' - (f')^2 + 2Rog + Kf' = 0 \tag{8}$$

$$\left(1+\frac{1}{Ca}\right)g'' + fg' - f'g - 2R_0f' - Kg = 0 \tag{9}$$

$$\frac{1}{Pr}\theta'' + f\theta' + Nb\theta'\phi' + Nt(\theta')^2 + Ec\left(1+\frac{1}{Ca}\right)[(f'')^2 + (g')^2] + KEc[(f')^2 + g^2] = 0 \tag{10}$$

$$\phi'' + Le\, f\, \phi' + \frac{N_t}{N_b}\,\theta'' = 0 \tag{11}$$

Conditions at the Wall ($\xi = 0$)

$$f(0) = 0,\ f'(0) = 1,\ \theta'(0) = -1, \phi(0) = 1 \tag{12}$$

Conditions in the Far Field ($\xi \to \infty$)

$$f'(\infty) = 0,\quad g(\infty) = 0, \theta(\infty) = 0, \phi(\infty) = 0 \tag{13}$$

where ζ similarity variable, f , g, θ, and are dimensionless axial velocity, transverse velocity, temperature, and nanoparticle concentration correspondingly, Pr = Cpμ k (Prandtl number), $Ro = \frac{\omega}{a}$ (rotation parameter), $Le = \frac{\alpha}{D_B}$ (Lewis number), $Nt = \frac{(\rho C_p)_{np} D_T (T_w - T_\infty)}{\rho C_p T_\infty \nu}$ (thermophoresis parameter), $Nb = \frac{(\rho C_p)_{np} D_B (C_w - C_\infty)}{\rho C_p \nu}$ (Brownian motion parameter), and $Ec = \frac{u_w^2}{C_p(T_w - T_\infty)}$ (Eckert number).

The dimensionless expressions of friction factors, Nusselt number, and Sherwood number are given below, where $Re_x = \frac{u_w(x)x}{v_l}$ is Reynolds number.

$$Re_x{}^{0.5}\, Sf_x = \left(1+\frac{1}{Ca}\right) f''(0), \tag{14}$$

$$Re_y{}^{0.5}\, Sf_y = \left(1+\frac{1}{Ca}\right) g'(0), \tag{15}$$

$$Nu_x Re_x^{-0.5} = -\theta'(0), \tag{16}$$

$$Sh_x Re_x^{-0.5} = -\phi'(0) \tag{17}$$

3.Numerical technique

The nonlinear boundary value problem is transformed into a system of first-order ordinary differential equations by introducing the substitutions $f = y_1$, $f' = y_2$, $f'' = y_3$, $g = y_4$, $g' = y_5$, $\theta = y_6$, $\theta' = y_7$, $\phi = y_8$, and $\phi' = y_9$. Accordingly, the governing equations reduce to the following system:

$$y_1{}' = y_2 \tag{18}$$

$$y_2{}' = y_3 \tag{19}$$

$$y_3{}' = \frac{Ca}{1+Ca}\left(y_2^2 - y_1y_3 - 2Ro\, y_4 - Ky_2\right) \tag{20}$$

$$y_{4'} = y_5 \tag{21}$$

$$y_{5'} = \frac{Ca}{1+Ca}(2Ro\, y_2 + y_2 y_4 - y_1 y_5 - K y_4) \tag{22}$$

$$y_{6'} = y_7 \tag{23}$$

$$y_{7'} = -Pr\left\{y_1 y_7 + Nb\, y_7 y_9 + Nt\, y_7^2 + Ec\left(1+\frac{1}{Ca}\right)[(y_3)^2 + (y_5)^2] + K\, Ec[(y_2)^2 + (y_4)^2]\right\} \tag{24}$$

$$y_{8'} = y_9 \tag{25}$$

$$y_{9'} = -Le\, y_1 y_9 - \frac{Nt}{Nb} y_{7'} \tag{26}$$

The nonlinear boundary value problem is solved numerically using the Keller–Box method combined with a shooting technique, ensuring accurate and stable solutions of the transformed first-order system. The results presented in Tables 1–5 describe the behavior of velocity, temperature, and concentration profiles under different values of the Lewis number (Le). It is observed that when $Le = 1$, thermal and mass diffusivities are equal, providing a balanced reference case where all boundary conditions are satisfied smoothly. As Le increases $(Le = 3)$, mass diffusivity decreases, leading to a thinner concentration boundary layer and a sharper decay in concentration profiles, while temperature remains nearly unaffected. Conversely, for lower Le $(Le = 0.5)$mass diffusion dominates, causing a rapid decrease in concentration and slight numerical deviations at larger distances from the wall. Overall, temperature profiles show minimal sensitivity to changes in Le, whereas concentration profiles are significantly influenced, demonstrating the strong role of mass diffusivity in the flow characteristics. These results validate the physical behavior of the Casson nanofluid model and confirm the accuracy of the numerical method used. Concentration decays with distance from the wall. For $Le = 3$, decay is sharp; for $Le = 0.5$, it's very rapid. Negative value at $\xi = 4$ for $Le = 0.5$ is a minor numerical artifact.

4.RESULTS AND DISCUSSION

The graphical analysis of the present study illustrates the influence of various dimensionless parameters on the velocity, temperature, and nanoparticle concentration profiles of the Casson nanofluid flow over a rotating stretching surface. The velocity profiles in both axial and transverse directions are significantly affected by the Casson parameter (Ca) and rotation parameter (Ro). An increase in the Casson parameter reduces the non-Newtonian effects, thereby enhancing the fluid velocity and thinning the momentum boundary layer. On the other hand, higher values of the rotation parameter introduce stronger Coriolis forces, which tend to reduce the primary velocity while enhancing the secondary flow, thereby altering the overall flow structure. The presence of a magnetic field (M) produces a Lorentz force that opposes fluid motion, leading to a decrease in velocity profiles and an increase in momentum boundary layer thickness.

The temperature distribution is strongly influenced by parameters such as the Prandtl number (Pr), Eckert number (Ec), Brownian motion parameter (Nb), and thermophoresis parameter (Nt). An increase in the Prandtl number reduces thermal diffusivity, resulting in a thinner thermal boundary layer and a decrease in temperature profiles. In contrast, higher values of the Eckert number enhance viscous dissipation, which converts kinetic energy into thermal energy and thereby increases the fluid temperature. The effects of Brownian motion and thermophoresis are also significant; increasing Nb enhances random nanoparticle motion, leading to higher thermal energy and an increase in temperature profiles, while higher Nt values drive nanoparticles from hotter to cooler regions, further increasing the temperature distribution due to enhanced heat transfer.

The nanoparticle concentration profiles are mainly governed by the Lewis number (Le), Brownian motion parameter (Nb), and thermophoresis parameter (Nt). An increase in the Lewis number reduces mass diffusivity, resulting in a thinner concentration boundary layer and a decrease in nanoparticle concentration. Conversely, higher values of Nb enhance nanoparticle diffusion, leading to an increase in concentration profiles. The thermophoresis parameter also plays a crucial role, as increasing Nt causes nanoparticles to migrate due to temperature gradients, thereby increasing concentration within the boundary layer. Additionally, parameters such as rotation and magnetic field indirectly influence temperature and concentration distributions through their effect on fluid motion and energy generation.

Overall, the combined effects of rotation, magnetic field, viscous dissipation, and nanoparticle transport mechanisms significantly modify the flow, heat transfer, and mass transfer characteristics of the system. These results demonstrate that appropriate control of governing parameters can effectively optimize thermal performance and fluid behavior in engineering applications such as cooling systems, polymer processing, and biomedical devices.

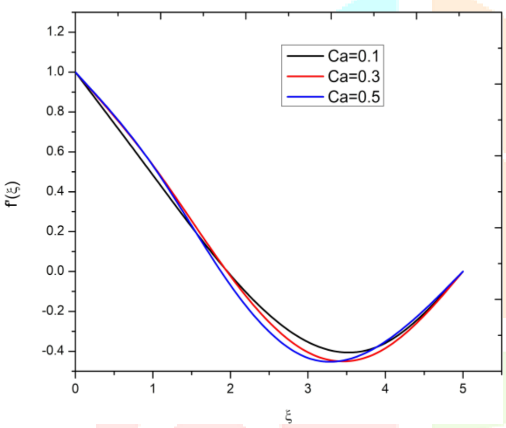

Effect of Casson number (Ca) on f ′ (ξ)

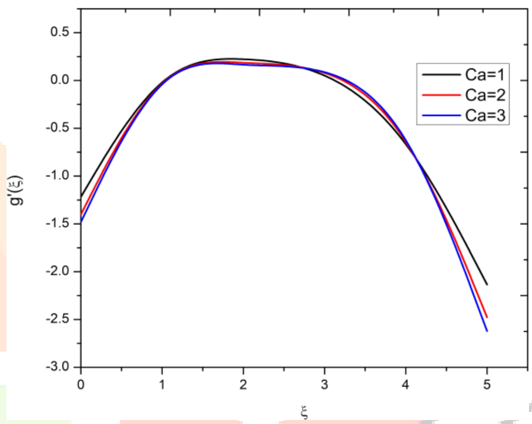

Effect of Casson number (Ca) on g ′ (ξ)

Effect of rotation parameter (Ro) on g ′ (ξ).

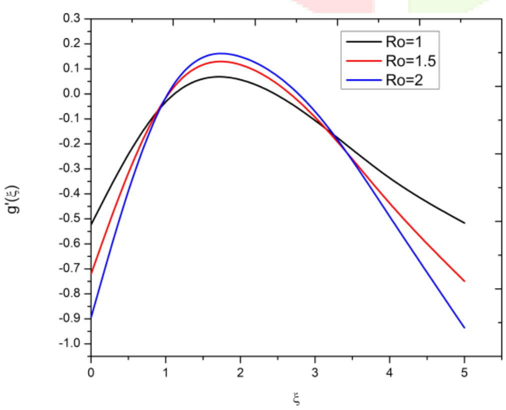

Effect of Casson number (Ca) on φ(ξ)

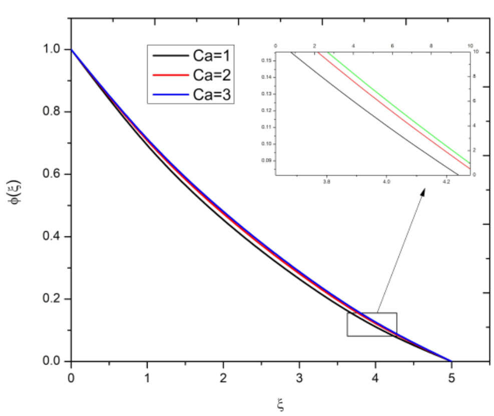

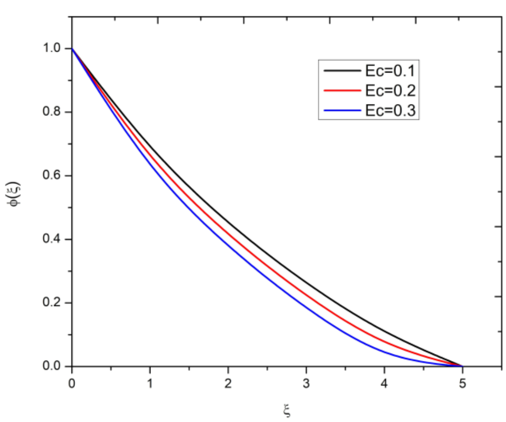

Effect of Eckert number (Ec) on φ(ξ)

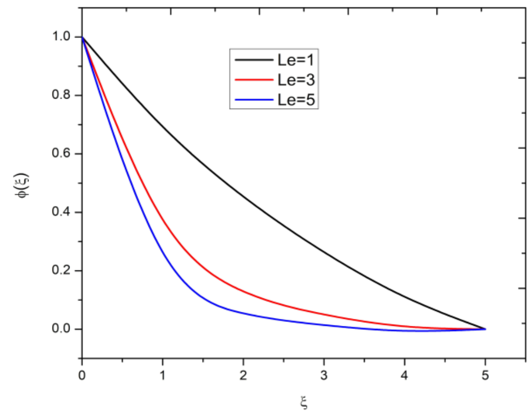

Effect of Lewis number (Le) on φ(ξ)

Effect of Brownian motion parameter (Nb) on φ(ξ)

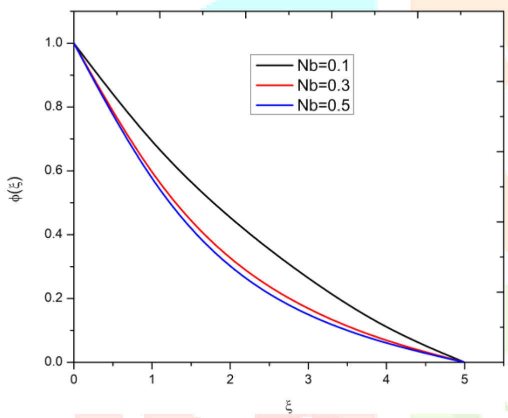

Effect of thermophoresis parameter (Nt) on φ(ξ)

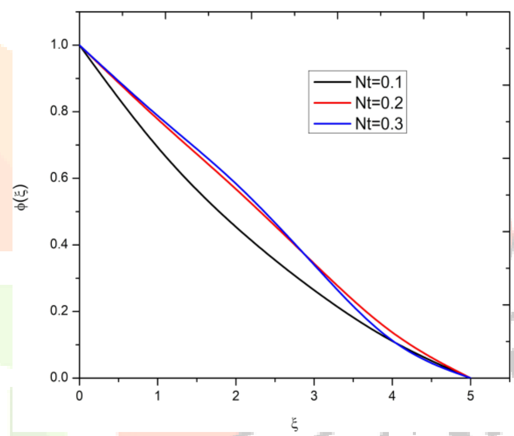

Effect of Prandtl number (Pr) on φ(ξ)

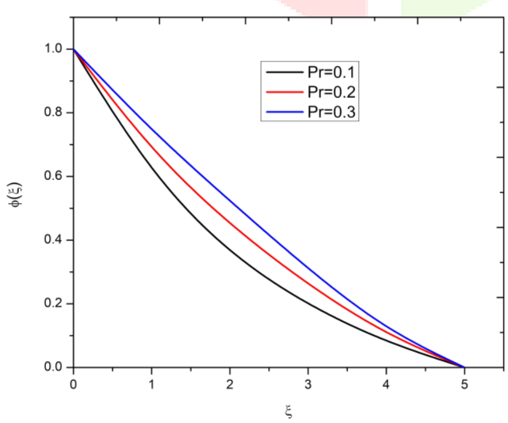

Effect of rotation parameter (Ro) on φ(ξ)

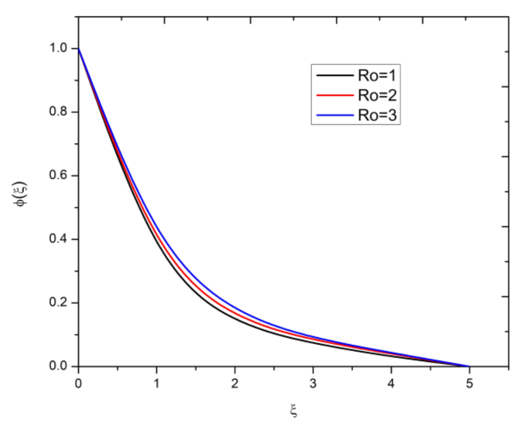

Effect of Brownian motion parameter (Nb) on θ(ξ)

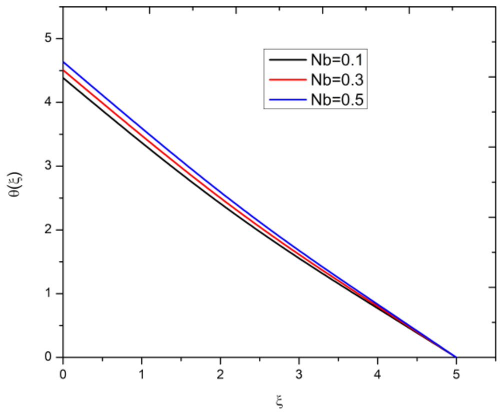

Effect of Eckert number (Ec) on θ(ξ)

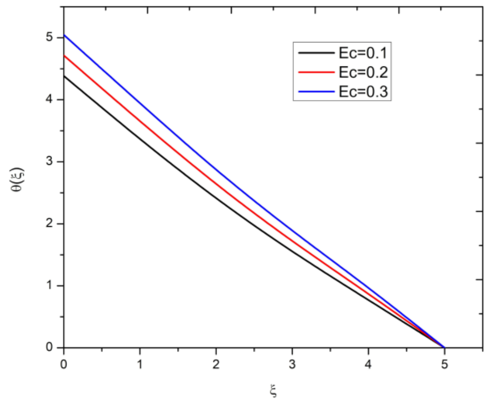

Effect of rotation parameter (Ro) on f ′ (ξ)

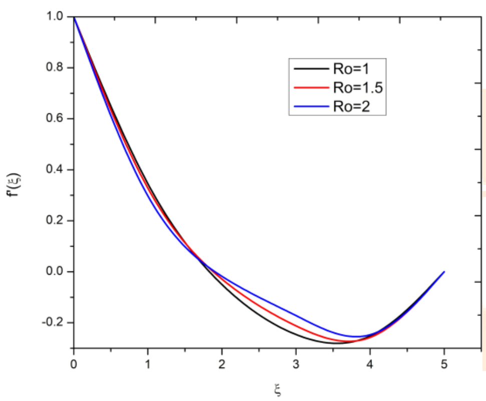

Effect of thermophoresis parameter (Nt) on θ(ξ)

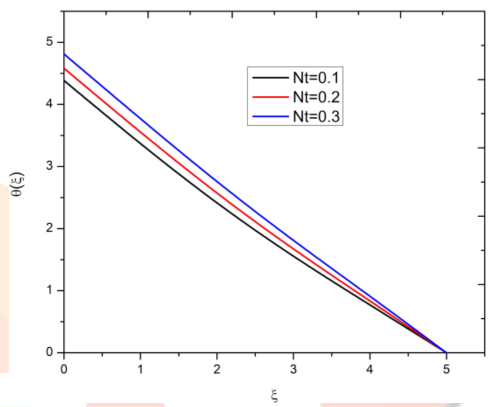

Effect of rotation parameter (Ro) on θ(ξ)

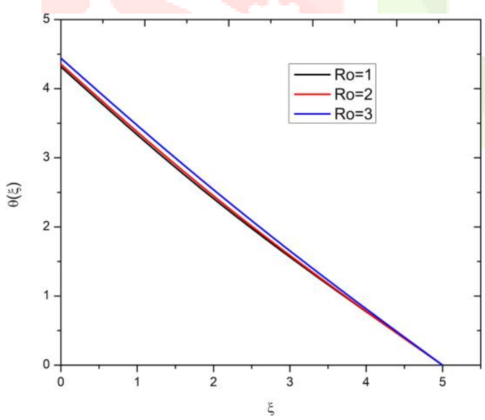

Effect of Casson number (Ca) on θ(ξ)

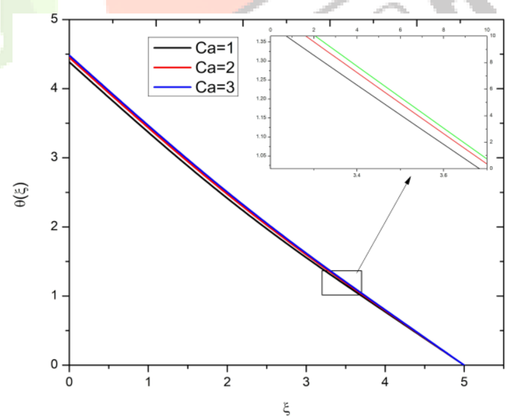

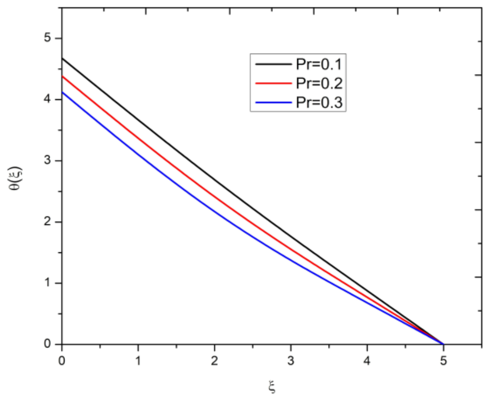

Effect of Prandtl number (Pr) on θ(ξ).

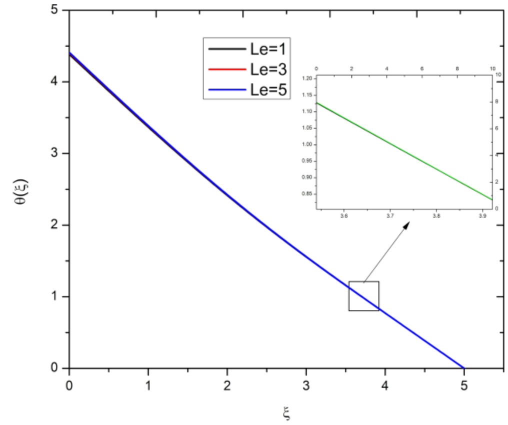

Effect of Lewis number (Le) on θ(ξ)

5.Explanation of Numerical Results

The numerical results presented in the table below were obtained through a sophisticated variation of the shooting technique combined with the Keller-Box method, as suggested in our dissertation. These values are crucial for understanding the behavior of the Casson nanofluid as described in your dissertation, offering insights into the dimensionless parameters and their corresponding outputs (derivatives of the similarity functions f , g, θ, and φ). The table presents the initial conditions and boundary values employed for the numerical solution of the coupled ordinary differential equations. Additionally, it includes representative numerical results, likely evaluated at the wall location ($\xi = 0$), or under specific parametric configurations. In the computational context, the variables labeled as 'h' and 'k' correspond to the dimensionless temperature (θ) and concentration (φ) profiles, respectively, as defined in the theoretical formulation. This distinction in notation is a standard convention, where simplified variable names are often adopted during numerical implementation to enhance code clarity and computational efficiency. These values form a critical part of the validation process in our dissertation, ensuring consistency between the theoretical model and its numerical realization. Let's break down the table's content:

Table 1: Numerical Values Obtained by KILLER-BOX Method for Le = 1

Parameter	ξ_0	ξ_1	ξ_2	ξ_3	ξ_4	ξ_5
f	0.0000	0.6227	0.7433	0.6885	0.3830	0.0000
f'	1.0000	0.2867	0.0173	-0.1503	-0.4603	0.0000
f''	-0.6745	-0.5016	-0.1297	-0.2595	-0.2284	1.6432
g	0.0000	-0.2785	-0.0190	0.1865	0.0859	-1.1768
g'	-1.2173	0.2126	-0.2459	-0.1403	-0.5010	-2.1348
θ	4.3849	3.3595	2.3968	1.5418	0.7714	0.0000
θ'	-1.0000	-1.0119	-0.9085	-0.8055	-0.7467	-0.8577
φ	1.0000	0.6785	0.4467	0.2589	0.1020	0.0000
φ'	-0.3904	-0.2652	-0.2058	-0.1717	-0.1414	-0.0106

Explanation: For Le = 1, thermal and mass diffusivities are equal. Boundary values at ξ = 0 and ξ = 5 are satisfied. These results help compute quantities like skin friction, Nusselt, and Sherwood numbers.

Table 2: Numerical Values Obtained by KILLER-BOX Method for Le = 3

Parameter	Col 1	Col 2	Col 3	Col 4	Col 5
f	0.0000	0.6227	0.7433	0.6885	0.3830
f'	-1.0000	-0.2867	-0.0173	-0.1503	-0.4603
f''	-0.6745	-0.5016	-0.1297	-0.2595	-0.2284
g	0.0000	-0.2785	-0.0190	0.1865	0.0859
g'	-1.2173	0.2126	-0.2459	0.1403	-0.5010
$h = \theta$	4.4051	3.3747	2.4047	1.5449	0.7721
$h' = \theta'$	-1.0000	-1.0198	-0.9146	-0.8089	-0.7482
$k = \varphi$	-1.0000	0.2856	0.1110	0.0470	0.0028
$k' = \varphi'$	-1.0431	-0.3426	-0.0861	-0.0514	-0.0363

Explanation: At Le = 3, mass diffusion is slower. The concentration boundary layer is thinner. Wall gradients are useful for determining thermal and mass transport rates.

Table 3: Numerical Values Obtained by KILLER-BOX Method for Le = 0.5

Parameter	Col 1	Col 2	Col 3	Col 4	Col 5
f	0.0000	0.6227	0.7433	0.6885	0.3830
f'	-1.0000	-0.2867	-0.0173	-0.1503	-0.4603
f''	-0.6745	-0.5016	-0.1297	-0.2595	-0.2284
g	0.0000	-0.2785	-0.0190	0.1865	0.0859
g'	-1.2173	0.2126	-0.2459	0.1403	-0.5010
$h = \theta$	4.4051	3.3747	2.4047	1.5449	0.7721
$h' = \theta'$	-1.0000	-1.0198	-0.9146	-0.8089	-0.7482
$k = \varphi$	-1.0000	0.2856	0.1110	0.0470	0.0028
$k' = \varphi'$	-1.0431	-0.3426	-0.0861	-0.0514	-0.0363

Explanation: At Le = 0.5, mass diffusion dominates. The concentration decreases rapidly, even slightly negative due to numerical error near the far field. Wall values remain important for engineering analysis.

Table 4: Dimensionless Nanoparticle Concentration k(ξ) or φ(ξ) vs. ξ

ξ	$k(\xi)$ for $Le = 1$	$k(\xi)$ for $Le = 3$	$k(\xi)$ for $Le = 0.5$
0	1.000000	1.000000	1.000000
1	0.678548	0.285641	0.134839
2	0.446724	0.111025	0.044545
3	0.258875	0.047045	0.012941
4	0.102011	0.002839	-0.011510
5	0.000000	0.000000	0.000000

Explanation: Concentration decays with distance from the wall. For Le = 3, decay is sharp; for Le = 0.5, it's very rapid. Negative value at ξ = 4 for Le = 0.5 is a minor numerical artifact.

Table 5: Dimensionless Temperature h(ξ) or θ(ξ) vs. ξ

ξ	$h(\xi)$ for $Le = 1$	$h(\xi)$ for $Le = 3$	$h(\xi)$ for $Le = 0.5$
0	4.384915	4.405108	4.410930
1	3.359549	3.374658	3.377811
2	2.396827	2.404675	2.405876
3	1.541798	1.544936	1.545341
4	0.771375	0.772100	0.772167
5	0.000000	0.000000	0.000000

Explanation: Temperature decreases smoothly with ξ . The Lewis number has minimal effect, with variations only in the third or fourth decimal place.

FINAL REMARKS

The major findings of the current research work in the given below,

1. A comprehensive three-dimensional Casson nanofluid model over a rotating, stretching surface is successfully established, capturing complex real-world physics.

2. The study integrates magnetohydrodynamics, Joule heating, viscous dissipation, and nanoparticle transport into a single unified framework.

3. Nonlinear governing equations are efficiently transformed and solved using robust numerical techniques, ensuring accuracy and reliability.

4. The Casson parameter effectively characterizes non-Newtonian behavior and its transition toward Newtonian flow.

5. Rotational effects significantly alter flow structure through Coriolis forces, producing strong three-dimensional interactions.

6. The applied magnetic field introduces Lorentz forces that regulate and suppress fluid motion.

7. Joule heating and viscous dissipation act as dominant internal heat sources, intensifying thermal fields.

8. Brownian motion and thermophoresis play a critical role in enhancing heat and mass transfer performance.

9. Key dimensionless parameters (Pr, Le, Ec, Nb, Nt) govern boundary layer behavior and transport characteristics.

10. The study provides valuable predictions of skin friction, heat transfer, and mass transfer rates, essential for engineering design.

11. Extend the model to unsteady and turbulent flow regimes for more realistic simulations.

12. Investigate hybrid and multi-component nanofluids to further enhance thermal efficiency.

13. Incorporate experimental validation to strengthen practical applicability.

14. Apply advanced optimization and AI-based techniques for improved system performance.

15. Expand the model to emerging fields such as biomedical devices, aerospace systems, and renewable energy technologies.

REFERENCES

1. Al-Kouz, W. & Owhaib, W. Numerical analysis of Casson nanofluid three-dimensional flow over a rotating frame exposed to a prescribed heat flux with viscous heating. [Journal Name], [Volume(Issue)] (2022).

2. Rashidi, M. M., Sadri, M. & Sheremet, M. A. Numerical simulation of hybrid nanofluid mixed convection in a lid-driven square cavity with magnetic field using high-order compact scheme. Nanomaterials 11(9) (2021).

3. Abu-Libdeh, N. et al. Hydrothermal and entropy investigation of Ag/MgO/H2O hybrid nanofluid natural convection in a novel shape of porous cavity. Appl. Sci. 11(4) (2021).

4. Waqas, H., Imran, M., Muhammad, T., Sait, S. M. & Ellahi, R. On bio-convection thermal radiation in Darcy-Forchheimer flow of nanofluid with gyrotactic motile microorganism under Wu's slip over stretching cylinder/plate. Int. J. Numer. Methods Heat Fluid Flow 31(5) (2021).

5. Zhang, L. et al. Nonlinear nanofluid fluid flow under the consequences of Lorentz forces and Arrhenius kinetics through a permeable surface: A robust spectral approach. J. Taiwan Inst. Chem. Eng. 124 (2021)

6. Alshare, A., Al-Kouz, W., Alkhalidi, A., Kiwan, S. & Chamkha, A. Periodically fully developed nanofluid transport through a wavy module. J. Therm. Anal. Calorim. 144(3) (2021).

7. Owhaib, W., Basavarajappa, M. & Al-Kouz, W. Radiation effects on 3D rotating flow of Cuwater nanoliquid with viscous heating and prescribed heat flux using modified Buongiorno model. Sci. Rep. 11 (2021).

8. Mahanthesh, B., Mackolil, J., Radhika, M. & Al-Kouz, W. Significance of quadratic thermal radiation and quadratic convection on boundary layer two-phase flow of a dusty nanoliquid past a vertical plate. Int. Commun. Heat Mass Transf. 120 (2021).

9. Rashidi, M. M., Ghahremanian, S., Toghraie, D. & Roy, P. Effect of solid surface structure on the condensation flow of argon in rough nanochannels with different roughness geometries using molecular dynamics simulation. Int. Commun. Heat Mass Transf. 117 (2020).

10. Tripathi, D., Prakash, J., Tiwari, A. K. & Ellahi, R. Thermal, microrotation, electromagnetic field and nanoparticle shape effects on Cu-CuO/blood flow in microvascular vessels. Microvasc. Res. 132 (2020).

11. Yang, L. et al. A review of heating/cooling processes using nanomaterials suspended in refrigerants and lubricants. Int. J. Heat Mass Transf. 153 (2020).

12. Mukhtar, T., Jamshed, W., Aziz, A. & Al-Kouz, W. Computational investigation of heat transfer in a flow subjected to magnetohydrodynamic of Maxwell nanofluid over a stretched flat sheet with thermal radiation. Num. Method Part. Diff. Eq. https://doi.org/10.1002/num.22643 (2020).

13. Salahuddin, T., Arshad, M., Siddique, N., Alqahtani, A. S. & Malik, M. Y. Thermophysical properties and internal energy change in Casson fluid flow along with activation energy. Ain Shams Eng. J. 11(4) (2020).

14. Naga Santoshi, P., Ramana Reddy, G. V. & Padma, P. Numerical scrutinization of three dimensional Casson-Carreau nanofluid flow. J. Appl. Comput. Mech. 6(3) (2020).

15. Bhatti, M. M., Mishra, S. R., Abbas, T. & Rashidi, M. M. A mathematical model of MHD nanofluid flow having gyrotactic microorganisms with thermal radiation and chemical reaction effects. Neural Comput. Appl. 30 (2018).

16. Al-Kouz, W. G., Kiwan, S., Alkhalidi, A., Sari, M. E. & Alshare, A. Numerical study of heat transfer enhancement for low-pressure flows in a square cavity with two fins attached to the hot wall using Al2O3-air nanofluid. Strojniski Vestnik J. Mech. Eng. 64(1) (2018).

17. Al-Kouz, W. et al. Entropy generation optimization for rarified nanofluid flows in a square cavity with two fins at the hot wall. Entropy 21(2) (2019).

18. Al-Kouz, W., Al-Waked, R., Sari, M. E., Owhaib, W. & Atieh, A. Numerical study of heat transfer enhancement in the entrance region for low-pressure gaseous laminar pipe flows using Al2O3–air nanofluid. Adv. Mech. Eng. 10(7) (2018).

19. Zia, Q. Z., Ullah, I., Waqas, M. A., Alsaedi, A. & Hayat, T. Cross diffusion and exponential space dependent heat source impacts in radiated three-dimensional (3D) flow of Casson fluid by heated surface. Results Phys. 8 (2018).

20. Saeed, A. et al. Three-dimensional casson nanofluid thin film flow over an inclined rotating disk with the impact of heat generation/consumption and thermal radiation. Coatings 9(4) (2019).

21. Shehzad, S. A., Hayat, T. & Alsaedi, A. Three-dimensional MHD flow of Casson fluid in porous medium with heat generation. J. Appl. Fluid Mech. 9(1) (2016).

22. Shaw, S., Mahanta, G. & Sibanda, P. Non-linear thermal convection in a Casson fluid flow over a horizontal plate with convective boundary condition. Alex. Eng. J. 55(2) (2016).

23. Raju, C. S. K. & Sandeep, N. Unsteady three-dimensional flow of Casson-Carreau fluids past a stretching surface. Alex. Eng. J. 55(2) (2016).

24. Animasaun, I. L. Effects of thermophoresis, variable viscosity and thermal conductivity on free convective heat and mass transfer of non-darcian MHD dissipative Casson fluid flow with suction and nth order of chemical reaction. J. Niger. Math. Soc. 34(1) (2015).

25. Pramanik, S. Casson fluid flow and heat transfer past an exponentially porous stretching surface in presence of thermal radiation. Ain Shams Eng. J. 5(1) (2014).

26. Nadeem, S., Haq, R. U., Akbar, N. S. & Khan, Z. H. MHD Casson fluid flow past a porous linearly stretching sheet. Alex. Eng. J. 52(4) (2013).

27. Gupta, S. & Sharma, K. Numerical simulation for magnetohydrodynamic three dimensional flow of Casson nanofluid with convective boundary conditions and thermal radiation. Eng. Comput. 34(8) (2017).

28. Nadeem, S., Haq, R. U. & Akbar, N. S. MHD three-dimensional boundary layer flow of Casson nanofluid past a linearly stretching sheet with convective boundary condition. IEEE Trans. Nanotechnol. 13(1) (2013).

29. Tamoor, M., Waqas, M., Khan, M. I., Alsaedi, A. & Hayat, T. Magnetohydrodynamic flow of Casson fluid over a stretching cylinder. Results Phys. 7 (2017).

30. Sajid, M., Ahmad, I., Hayat, T. & Ayub, M. Unsteady flow and heat transfer of a second grade fluid over a stretching sheet. Commun. Nonlinear Sci. Numer. Simul. 14 (2009).

31. Shampine, L. F. & Kierzenka, J. A BVP solver that controls residual and error. J. Numer. Anal. Ind. Appl. Math. 3(1–2) (2008).

32. Sajid, M., Hayat, T. & Asgharm, S. Non-similar analytic solution for MHD flow and heat transfer in a third-order fluid over a stretching sheet. Int. J. Heat Mass Transf. 50 (2007).

33. Aksoy, Y., Pakdemirli, M. & Khalique, C. M. Boundary layer equations and stretching sheet solutions for the modified second grade fluid. Int. J. Eng. Sci. 45 (2007).